11

Use of Radiobiological Modeling in Treatment Plan Evaluation and Optimization of Prostate Cancer Radiotherapy

Panayiotis Mavroidis[1], Dimos Baltas[2],
Bengt K. Lind[1] and Nikos Papanikolaou[3]
[1]*Department of Medical Radiation Physics*
Karolinska Institutet and Stockholm University
[2]*Department of Medical Physics & Engineering, Strahlenklinik,*
Klinikum Offenbach GmbH
[3]*Department of Radiological Sciences*
University of Texas Health Science Center, San Antonio, Texas
[1]*Sweden*
[2]*Germany*
[3]*USA*

1. Introduction

There are many tools available that are used to evaluate a radiotherapy treatment plan, such as isodose distribution charts, dose volume histograms (DVH), maximum, minimum and mean doses of the dose distributions as well as DVH point dose constraints. All the already mentioned evaluation tools are dosimetric only without taking into account the radiobiological characteristics of tumors or OARs. It has been demonstrated that although competing treatment plans might have similar mean, maximum or minimum doses they may have significantly different clinical outcomes (Mavroidis et al. 2001). For performing a more complete treatment plan evaluation and comparison the complication-free tumor control probability (P_+) and the biologically effective uniform dose ($\overline{\overline{D}}$) have been proposed (Källman et al. 1992a, Mavroidis et al. 2000). The $\overline{\overline{D}}$ concept denotes that any two dose distributions within a target or OAR are equivalent if they produce the same probability for tumor control or normal tissue complication, respectively (Mavroidis et al. 2001).
In this chapter, the importance of the $P-\overline{\overline{D}}$ diagrams is illustrated. These diagrams provide important information by combining the radiobiological data of the organs involved with the dosimetric information of the delivered dose distribution (Mavroidis et al. 2010). It would increase the flexibility and clinical application of the P_+ index if in its original definition the different terms related to the tumor control and normal tissue complication probabilities were accompanied by some weighting factors, which could be adjustable by the clinicians depending on the important of the different clinical endpoints used (Mavroidis et al. 2011). In practice the P_+ index finds the pure benefit from the treatment by subtracting the normal tissue complication probabilities from the tumor control probability.

In clinical practice, there are not different weighting factors that are applied but there are risk thresholds (usually 5-10%) for every organ at risk, which should not be exceeded (Mavroidis et al. 2011). So, in order to classify the different treatment plans one can select the dose level that satisfies these demands imposed by the normal tissues risk thresholds and compare the expected tumor control rates at this dose level.

By using the $\overline{\overline{D}}$ concept on the dose axis, the control and complication probabilities of the target and OARs can be examined individually. Due to the fact that different plans generally deliver different mean doses to the target for the same control rate, the use of the target mean dose as a dose scaling basis is not suitable since the expected response rates induced by the treatment to the rest of the involved organs cannot be easily compared using this scale. The major advantage is that the $\overline{\overline{D}}$ concept forces the total control probabilities of different plans to coincide and the comparison of the response curves becomes much simpler than when the mean target dose is used (Mavroidis et al. 2001).

The results and conclusions of this chapter are strongly dependent on the accuracy of the radiobiological models and the parameters describing the dose-response relation of the different tumours and normal tissues (Mavroidis et al. 2007). However, it is known that all the existing models are based on certain assumptions or take into account certain only biological mechanisms. Furthermore, the determination of the model parameters expressing the effective radiosensitivity of the tissues is subject to uncertainties imposed by the inaccuracies in the patient setup during radiotherapy, lack of knowledge of the inter-patient and intra-patient radiosensitivity and inconsistencies in treatment methodology (Buffa et al. 2001, Fenwick & Nahum 2001). Consequently, the determined model parameters and the corresponding dose-response curves are characterized by confidence intervals. In the present analysis, most of the tissue response parameters have been taken from recently published clinical studies, where these parameter confidence intervals has been reduced significantly (e.g. uncertainty of around 5% in the determination of D_{50}). So, the expected response of a tissue is known with some uncertainty, which can be considered clinically acceptable (Mavroidis et al. 2007).

In this chapter, the treatment plans were optimized using conventional physical criteria like dose volume histograms, isodose charts, DVH point constraints, target prescribed doses and OAR tolerance doses. However, the developed treatment plans were evaluated radiobiologically using the radiation sensitivities of the respective organs involved in each case. The expected normal tissue complications were estimated against the optimum target dose using radiobiological plots. Just as a dose volume histogram is a good illustration of the volumetric dose distribution delivered to the target and OAR in the patient, so is the radiobiological evaluation plot as a measure of the expected clinical outcome. The dose-response diagrams in conjunction with the dosimetric diagrams provide a more thorough viewpoint of the examined treatment plans.

2. Organ delineation and treatment planning using CT vs. CT-MRI images during in prostate cancer radiotherapy

Traditionally, targets and organs-at-risk (OAR) are anatomically delineated on computed tomography (CT)-images in prostate cancer treatment planning. However, in CT the sensitivity of visualizing extracapsular involvement is lower than in magnetic resonance imaging (MRI), which provides much more detailed information. MRI can superbly

demonstrate the internal prostatic anatomy, prostatic margins and the extent of prostatic tumors (Chen et al. 2004, Parker et al. 2003, Rørvik et al. 1993, Villeirs et al. 2007). It has been shown that an important decrease in the inter-observer delineation variation, as well as a significant decrease in the clinical target volume (CTV) may be resulted in by the use of fused MRI-CT images (Villeirs et al. 2005). Using MRI for delineation, the reduced prostate-target volume is associated with a reduction of the rectal wall being irradiated, which may result in fewer rectal and urological complications (Rasch et al. 1999). More specifically, the use of axial and coronal MR scans, in localized prostate carcinoma treatment planning results in a better coverage of the prostate and a reduction of the volume of the rectum irradiated to high doses (Debois et al. 1999).

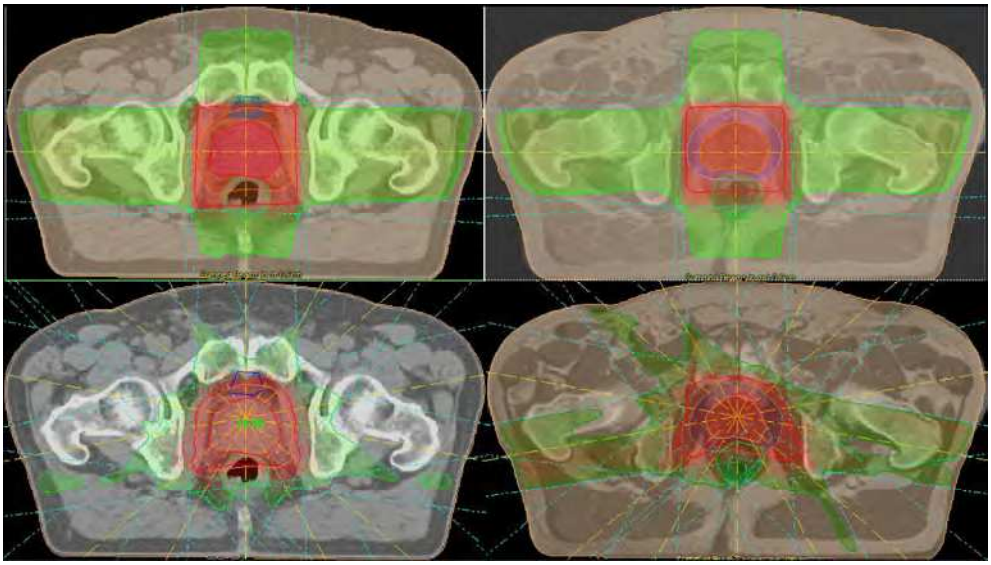

Fig. 1. The reference CT (left) and fused CT-MRI (right) slices of a prostate cancer patient is shown for the 3D-CRT (upper) and MLC-based IMRT (lower) treatment plans in the transverse plane. The delineations of the anatomical structures involved were performed based on the CT and MRI images and they are illustrated together with the dose distributions delivered to the patient (Tzikas et al. 2011) (published with permission from: Tzikas et al. Investigating the clinical aspects of using CT vs. CT-MRI images during organ delineation and treatment planning in prostate cancer radiotherapy. Technology in Cancer Research and Treatment, Vol.10, pp. 235 and 236, 2011, Adenine Press, http://www.tcrt.org).

In the present analysis, the respective CT and MRI images at treatment position were acquired for 10 prostate cancer patients (Tzikas et al. 2011). For each patient the separate CT and MRI images were used to delineate the Clinical Target Volume (CTV), which includes the prostate gland and the seminal vehicles. During treatment planning, the MRI and CT images were fused. The PTV was produced by adding to the CTV 1.0 cm margin in all directions apart from that towards rectum, which was 0.6 cm. So, 2 PTVs were produced for each patient based on the CT and MRI images. The comparison of the prostate cancer treatment plans in terms of isodose lines and dose volume histograms (DVH) is shown in

Figs. 1 and 2. Furthermore, individual dose-response curves and P_+ - $\bar{\bar{D}}_B$ plots of the CT and CT-MRI based treatment plans are presented in Fig. 3 for the CRT (left) and IMRT (right) radiation modalities, respectively.

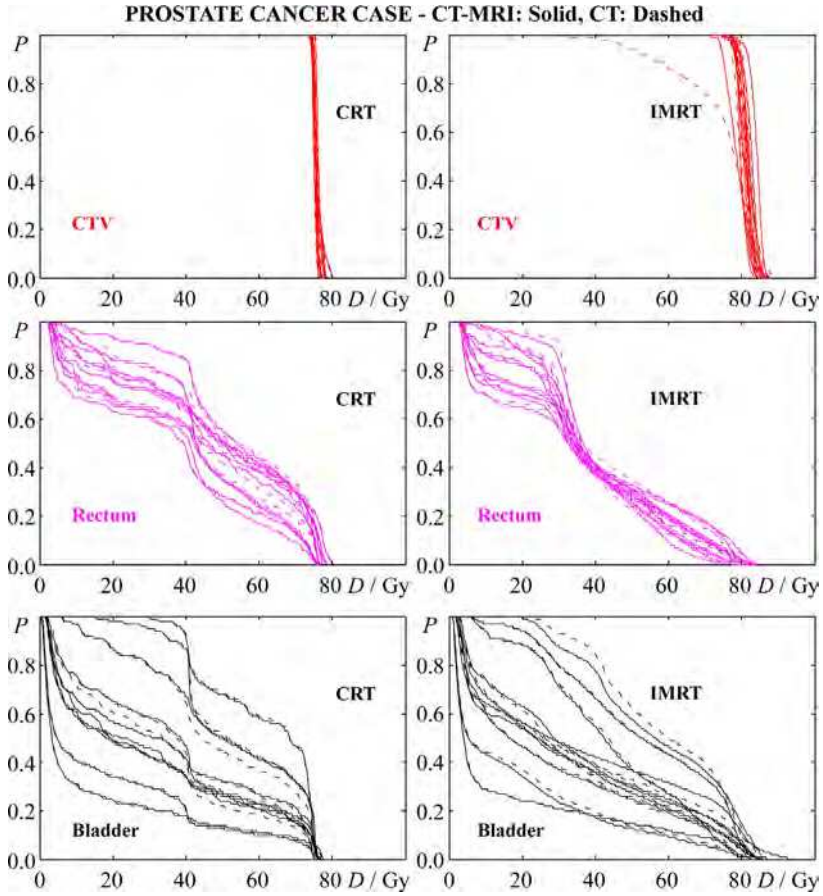

Fig. 2. The dose volume histograms (DVHs) of the CTV, rectum and bladder are presented in the upper, middle and lower diagrams, respectively for the CRT (left) and IMRT (right) treatment plans, which were optimized based on the CT and fused CT-MRI images, separately.

For the treatment plans of the CRT treatment modality, which were produced based on the CT images, at the clinical dose prescription the average P_+ value is 15.9% for a mean dose ($\bar{D}_{CTV}$) and a biologically effective uniform dose ($\bar{\bar{D}}_B$) to the CTV of 75.5 Gy. The average total control probability, P_B is 26.5% and the average total complication probability, P_I is 10.5%. Similarly, for the treatment plans that were produced based on the fused CT-MRI images, the average P_+ value is 17.5% for the same $\bar{D}_{CTV}$ and $\bar{\bar{D}}_B$. The average P_B the same with that of the treatment plans that were produced using CT images alone (26.5%) and the average P_I is 8.9%. However, at the dose level of the individual dose distributions that the

complication-free tumor control gets optimum, for the CT-based treatment plans, the P_+ value becomes 42.5% for a $\bar{\bar{D}}_B$ of 86.4 Gy having average P_B = 80.0% and average P_I = 37.4%, whereas for the CT-MRI-based treatment plans, the P_+ value becomes 46.7% for a $\bar{\bar{D}}_B$ of 86.7 Gy having an average P_B = 80.6% and an average P_I by 33.8%.

For the treatment plans of the IMRT treatment modality, which were produced based on the CT images, at the clinical dose prescription, the P_+ value is 52.5% for $\bar{D}_{CTV}$ = 81.0 Gy and $\bar{\bar{D}}_B$ = 80.8 Gy. The average P_B is 57.1% and the average P_I is 4.7%. Similarly, for the CT-MRI-based treatment plans, the P_+ value is 53.4% for $\bar{D}_{CTV}$ = 80.8 Gy and $\bar{\bar{D}}_B$ = 80.5 Gy. The average P_B = 58.6% and the average P_I = 5.2%. However, at the dose level that maximizes the complication-free tumor control for the CT-based plans, the P_+ value becomes 74.7% for a $\bar{\bar{D}}_B$ of 91.5Gy having P_B = 90.0% and P_I = 15.3%, whereas for the CT-MRI-based plans, the P_+ value remains the same for a higher $\bar{\bar{D}}_B$ by 0.6 Gy. The corresponding average P_B = 90.2%, whereas the average P_I = 15.4%.

If the CT-based treatment plans were applied to calculate the dose in target and OARs that were produced using the fused CT-MRI images then the average differences would be almost zero in the case of CRT radiation modality, whereas in the case of IMRT radiation modality the P_+ value would become 2.1% lower, the average P_B would be lower by 2.1% while the average P_I would remains the same.

Observing the diagrams in Fig. 3 it is apparent that the clinically established dose prescription, which corresponds to a certain uniform dose in the CTV deviates from the optimal dose level that is indicated by the radiobiological evaluation. For example, the clinically prescribed dose level is lower than the optimum level by $\Delta\bar{\bar{D}}$ = 8-14 Gy. According to these findings, it is expected that a small increase in the dose prescription will slightly increase the complication rate but it will also be accompanied by a significant increase in the control rate. As shown in Fig. 3, a margin of improvement can be observed while the individual normal tissue responses are kept below the limit of 10% as indicated by the horizontal crossed bar.

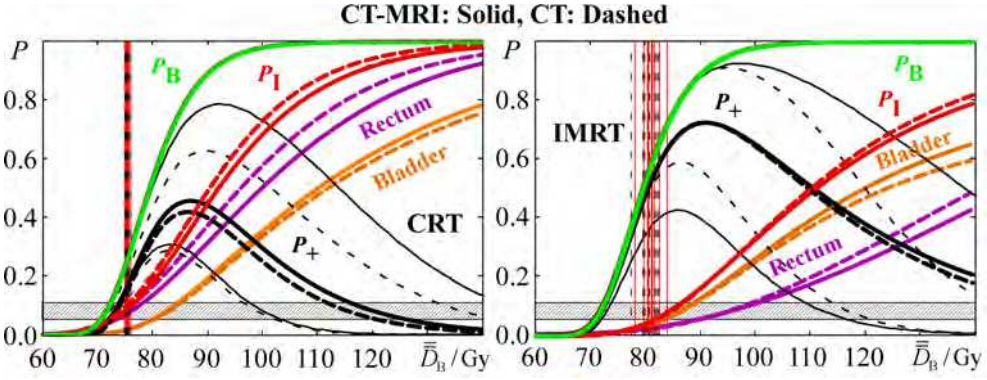

Fig. 3. The dose-response curves of the CTV / total control probability, P_B, bladder, rectum, total complication probability, P_I and complication-free tumor control probability, P_+ are presented for the CRT and IMRT treatment plans, which were optimized based on the CT and fused CT-MRI images, separately. The horizontal crossed bar indicates the 5-10% response probability region. The vertical lines represent the prescribed dose levels of the individual patients.

It is worth of noticing that the OAR with the highest risk for complications is rectum in the case of CRT and bladder in the case of IMRT (Fig. 3). This observation confirms previous reports that one of the most important advantages of IMRT over 3D-CRT is the ability of sparing the rectal wall reducing the development of late toxicity. In Fig. 3, it is shown that the results vary considerably among the patients as indicated by the thin P_+ lines.
For the CRT treatment plans, the response probabilities of CTV and bladder from the CT and fused CT-MRI based treatment plans do not differ significantly (p=0.87 and p=0.49, respectively), whereas those of rectum differ significantly (p=0.02) (Tzikas et al 2011). On the other hand, for the IMRT treatment plans, the response probabilities of all the structures (CTV, bladder and rectum) do not differ significantly between the two sets of plans (p=0.68, p=0.59 and p=0.34, respectively). The improvement that results in by the use of fused CT-MRI images in the overall effectiveness of the CRT plans is statistically significant (p=0.03), which is mainly caused by the statistically significant sparing of the OARs (p=0.03 for P_I). In the IMRT treatment plans this improvement does not get statistically significant. This stems from the fact that IMRT radiation has to capability of producing highly conformal dose distributions that can spare already from the beginning very well the OARs.
In the future, target volumes could be reduced by both CT/MRI co-registration and dose painting using MR spectroscopy (Claus et al. 2004, Hou et al. 2009, Scheidler et al. 1999, Weinreb et al. 2009). These ongoing improvements and developments in radiotherapy treatment planning are leading to treatments which offer both better tumour volume coverage, and are minimizing the risk of treatment-related complications (Beasley et al. 2005). These changes should allow the escalation in dose delivered to the tumour volume with the potential for increased cure rates.

3. Daily megavoltage CT registration on adaptive Helical Tomotherapy

In treatments where the organs-at-risk (OARs) are close to the clinical target volume (CTV), the accuracy of the delivered dose is critical. The existence of an accurate patient positioning process is a prerequisite for ensuring agreement between planned and delivered dose distributions (Creutzberg et al. 1993, Mitine et al. 1991). Patient setup inaccuracies can lead to variations in dose delivery and under-dosage of tumors or over-dosage of normal tissues, which can result in a considerable reduction of local tumor control and/or increase of side effects, respectively (Mavroidis et al. 2011).
Helical Tomotherapy (HT) is characterized by dose distributions of high dose conformity (Mackie et al. 1999, Webb 2000). Presently, the Planned Adaptive module of the Tomotherapy software is used to correct dose discrepancies that may occur during treatment delivery. The comparison of the delivered and planned fractional dose distributions can be made in several treatment fractions. To measure the extent of the patient setup deviation on a helical tomotherapy machine, a megavoltage computed tomography (MVCT) scan has been developed for daily correction of patient positioning (Boswell et al. 2006, Meeks et al. 2005, Welsh et al. 2006). Due to the highly conformal distributions that can be obtained with HT any discrepancy between the planned and delivered dose distributions may result in the degradation of the curative power and effectiveness of the treatment (Löf et al. 1995). Consequently, there is a need to measure those differences in terms of a change in the expected clinical outcome. The present analysis performs assessment of the clinical effectiveness of the delivered treatment by interpreting the dosimetric characteristics of the different dose distributions and translating them into expected rates of tumor control and normal tissue complications.

For each of the examined patients, a Helical Tomotherapy plan was developed and subsequently the calculated dose distributions with and without patient setup correction were compared by using physical and radiobiological measures (Mavroidis et al. 2011). The corresponding cumulative dose distributions, which are determined by adding the delivered fractional dose distributions, are calculated for the entire course of radiation therapy (Fig. 4).

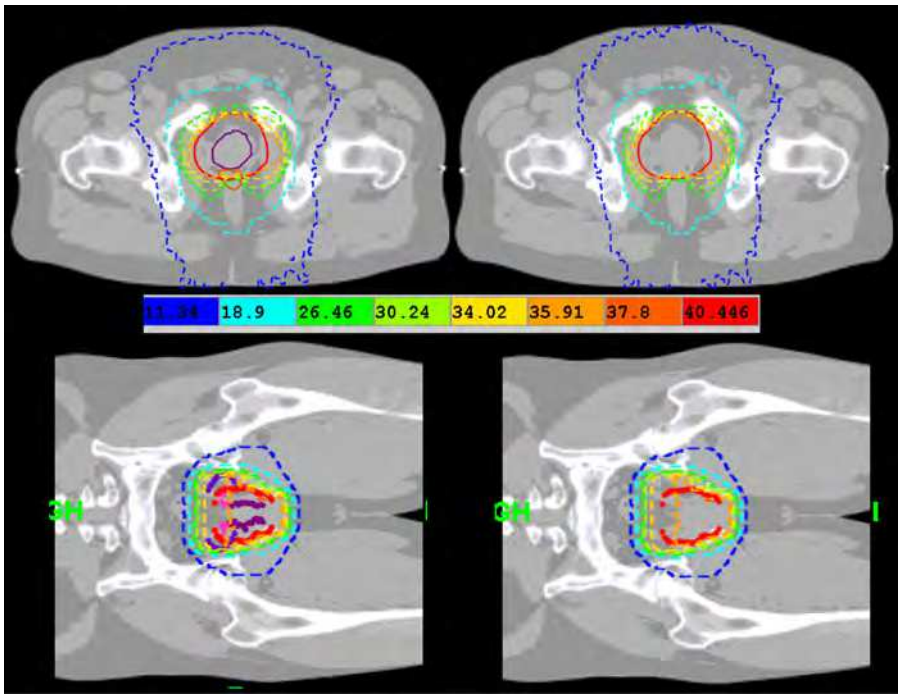

Fig. 4. The reference CT slices of a prostate cancer patient are shown in the transverse and coronal planes for the Helical Tomotherapy dose distributions with (left) and without (right) patient setup correction. In each case, the dose values of the isodose lines are also presented.

In this investigation each patient has a reference kilovoltage CT (kVCT) that was used for the development of the treatment plan. For each fraction, a pre-treatment verification megavoltage CT (MVCT) was obtained in the tomotherapy unit to assess setup accuracy. In order to evaluate the dosimetric effect of setup correction in Helical Tomotherapy, two different cumulative dose distributions were analyzed for the examined clinical cases. One cumulative dose distribution was calculated by adding up the separate delivered fractional dose distributions with setup correction. In this set of merged images, a mutual information based registration (that considered translational and rotational only corrections) was performed between the reference kVCT and the pre-treatment MVCT for each fraction based on anatomical landmarks. The other cumulative dose distribution was computed by adding up the delivered fractional dose distributions as calculated on the daily MVCT, without applying any positional corrections from the daily MVCT-kVCT co-registration. The dose distributions with and without patient repositioning were computed and the final dose volume histograms (DVHs) for both dose calculations were compared (Fig. 5).

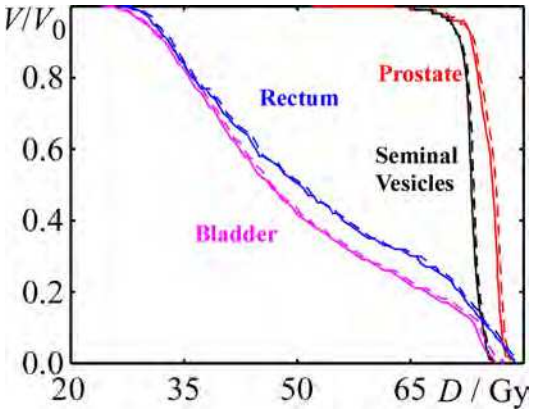

Fig. 5. The dose volume histograms (DVHs) of the targets (Prostate, Seminal Vesicles) and organs at risk (bladder, rectum) are illustrated. The solid lines correspond to the dose distribution with setup correction, whereas the dashed lines correspond to the dose distribution without setup correction (Mavroidis et al. 2011) (published with permission from: Mavroidis et al. Radiobiological and dosimetric analysis of daily megavoltage CT registration techniques on adaptive radiotherapy with Helical Tomotherapy. Technology in Cancer Research and Treatment, Vol.10, pp. 9, 2011, Adenine Press, http://www.tcrt.org).

For this dose prescription of the dose distributions with and without setup correction, the complication-free tumor control probabilities, P_+ are 10.9% and 11.9% for mean doses to the ITV ($\bar{D}_{ITV}$) of 74.7 Gy and 75.2 Gy and biologically effective uniform doses to the ITV ($\bar{\bar{D}}_B$) of 75.2 Gy and 75.4 Gy, respectively. The corresponding total control probabilities, P_B are 14.5% and 15.3%, whereas the total complication probabilities, P_I are 3.6% and 3.4%, which are almost equal to the response probabilities of the rectum (3.6% and 3.4%, respectively). At the dose level of the dose distributions with and without setup correction that maximizes the P_+ index ($\bar{D}_{ITV}$ = 90.0 Gy), the P_+ values are 55.9% and 57.7%, respectively.

Response probability	Clinical Dose Prescription		Optimum Dose Prescription	
	With setup correction	W/o setup correction	With setup correction	W/o setup correction
GTV (%)	15.5	+ 0.8	85.2	- 1.0
Seminal Vesicles (%)	93.6	+ 0.2	99.5	0.0
Bladder (%)	0.1	0.0	5.1	- 0.3
Rectum (%)	3.6	- 0.2	25.0	- 2.6
P_+ (%)	**10.9**	**+ 1.0**	**55.9**	**+ 1.8**
P_B (%)	**14.5**	**+ 0.8**	**84.7**	**- 1.0**
P_I (%)	**3.6**	**- 0.2**	**28.8**	**- 2.8**
$\bar{D}_{ITV}$ (Gy)	**74.7**	**+ 0.5**	**90.0**	**0.0**
$\bar{\bar{D}}_B$ (Gy)	**75.2**	**+ 0.2**	**90.6**	**- 0.4**

Table 1. Summary of the radiobiological comparison.

As it is shown in Fig. 6, the expected complication-free tumor control for the dose distributions with setup correction is equivalent or worse than the delivered dose distributions without setup correction. The reason is that the HT TPS does not have the possibility of performing radiobiological treatment plan optimization, which means that the planned dose distributions could not be produced using the maximum P_+ as objective. By examining the tumor control and normal tissue complication probabilities separately it can be observed that the dose distributions with setup correction have the same or higher response probabilities than the dose distributions without setup correction. However, for normal tissues the classification of the dose distributions with and without setup correction seems to be more sensitive and it varies depending on the case. In all the cases, the ITV is irradiated almost iso-effectively by the delivered dose distributions with and without patient setup correction. This is supported by the tumor control probabilities, P_B that are presented in Table 1 (Mavroidis et al. 2011). On the other hand, the setup uncertainties produce higher normal tissue complications when the OARs move into the high dose region or lower expected responses when the OARs move away from the high dose region.
As far as tissues of parallel internal organizations are concerned, dose inhomogeneity does not affect significantly their response, which is mainly determined by the mean dose. In this case, although the variation of a given dose distribution may be large, the $\bar{\bar{D}}$ value does not deviate much from the corresponding mean dose, $\bar{D}$, due to the low relative seriality value characterizing such a tissue.

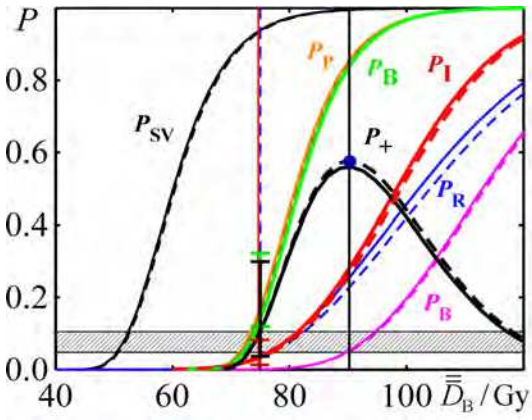

Fig. 6. The dose-response curves that are derived from the radiobiological evaluation of the dose distributions are plotted using $\bar{\bar{D}}$ on the dose axis. The horizontal crossed bar indicates the 5-10% response probability region. The solid and dashed vertical lines indicate the dose levels of the dose distributions with and without setup correction, respectively. The vertical error bars indicate the confidence intervals of the corresponding dose-response curves due to the uncertainties of the radiobiological parameters. The solid lines correspond to the dose distribution with setup correction, whereas the dashed lines correspond to the dose distribution without setup correction.

In Fig. 6, the clinically established dose prescription (solid and dashed vertical lines), deviates from the optimal dose level that is indicated by the radiobiological evaluation. With a small increase in the dose prescription an increase in the complication-free tumor control, P_+ can be achieved because the gain in tumor control is larger than the increment in normal tissue complications until a balance is reached. The dashed vertical line indicates the dose prescription, which intersects with the total complication probability of 10%. Because of these points the clinically prescribed dose level is lower than the optimum level by a $\Delta\bar{\bar{D}}$ of about 15.0 Gy.

In the DVH diagram (Fig. 5) it is observed that a significantly higher dose is delivered to the ITV compared to the OARs, which leads to response curves that are well separated from those of the targets as shown in Fig. 6. The width of the P_+ curve expresses the separation between the response curves of the targets and those of the OARs. At the same time, the most effective dose distribution is indicated, since it generates a higher value of P_+. The more conformal a treatment technique is the more precise and accurate the patient setup process should be. In these techniques the dose distribution is so well matched with the radiosensitivity map of the clinical case that a small misalignment in the setup can rapidly reduce the effectiveness of the delivered therapy. The quality of a treatment does not only depend on the conformity of the applied technique but also on the quality of the supporting services.

4. Radiobiological evaluation of Helical Tomotherapy and MLC-based IMRT treatment plan

Helical Tomotherapy (HT) is a radiation modality that is capable of producing high conformity dose distributions that may be superior than other IMRT techniques (Mackie et al. 1999, Webb 2000). A unique radiation delivery method is employed by HT, which delivers radiation helically through fifty-one projections per rotation. Although HT can produce very conformal dose distributions, it is still unknown how much the effectiveness of the resulted dose distributions differs from that of other radiation therapy modalities such as that of the MLC-based step-and-shoot IMRT. Consequently, the goal of this analysis is to compare IMRT treatment plans generated using MLC-based step-and-shoot IMRT and HT technology based on radiobiological measures, using representative prostate cancer cases. For each case, two sets of treatment plans have been developed (IMRT and HT). A parallel physical and radiobiological evaluation was carried out to assess the different treatment plans. The implemented radiobiological procedure estimates the probability to achieve tumour control without complications based on the knowledge of the dose-response relations of the tumours and organs-at-risk (Emami et al. 1991, Mavroidis et al. 2003, 2005, Ågren 1995).

Fig. 7 illustrates the dose distributions of a conventional, a conformal (CRT), an MLC-based IMRT and a HT treatment plan, of a prostate cancer case, in the form of isodose curves in transverse and coronal views, respectively (Mavroidis et al. 2007). According to the isodose curve distributions, it appears that the HT plan produces slightly lower inhomogeneity inside the ITV as compared to the MLC-based IMRT and very similar dose spread outside the ITV. The MLC-based IMRT radiation modality delivers higher mean doses to the GTV, lymph nodes and bladder and a lower dose to the rectum as compared to the HT (Table 2).

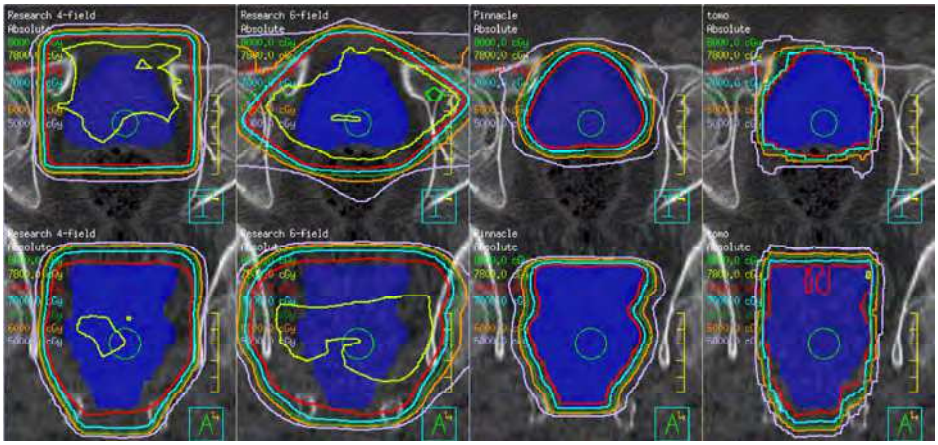

Fig. 7. The reference CT slice of a prostate cancer patient is shown for the treatment plans of four radiation modalities in the transverse and coronal planes. The anatomical structures involved are illustrated together with the dose distributions delivered to the patient.

Tissue	GTV	Lymph nodes	Bladder	Rectum
Helical Tomotherapy				
P_{Tomo} (%)	39.3	98.0	1.0	2.9
$\bar{\bar{D}}_{\text{Tomo}}$ (Gy)	74.8	74.8	61.6	59.6
$\bar{D}_{\text{Tomo}}$ (Gy)	74.9	74.8	39.7	34.8
SD_{Tomo}	0.9	0.5	20.6	17.6
$D\text{max}_{\text{Tomo}}$	78.3	77.9	77.9	77.9
$D\text{min}_{\text{Tomo}}$	71.2	73.2	8.3	6.7
MLC-based IMRT				
P_{IMRT} (%)	44.1	98.4	1.4	1.3
$\bar{\bar{D}}_{\text{IMRT}}$ (Gy)	75.6	75.9	62.1	57.7
$\bar{D}_{\text{IMRT}}$ (Gy)	75.6	75.9	41.8	34.3
SD_{IMRT}	0.7	0.3	20.2	16.1
$D\text{max}_{\text{IMRT}}$	77.5	77.1	76.7	74.7
$D\text{min}_{\text{IMRT}}$	72.8	74.7	7.9	4.4

Table 2. Summary of the radiobiological evaluation of the Helical Tomotherapy and IMRT treatment plans.

For the applied dose prescription the complication-free tumor control probability (P_+) value is 34.7% for the HT for a mean dose to the ITV ($\bar{D}_{ITV}$) of 74.9 Gy and biologically effective uniform dose to the ITV ($\bar{\bar{D}}_B$) of 74.8 Gy. The total control probability (P_B) is 38.5% and the total complication probability (P_I) is 3.8%. Similarly, of the MLC-based IMRT the P_+ value is 40.8% for $\bar{D}_{ITV}$ = 75.7 Gy and $\bar{\bar{D}}_B$ = 75.6 Gy. The P_B = 43.4% and the P_I = 2.6% (Mavroidis et al 2007). However, if we optimize the dose level of the dose distributions in order to maximize the complication-free tumor control then for the HT, the P_+ value becomes 68.7% for a $\bar{\bar{D}}_B$ of 86.0 Gy stemming from P_B = 87.8% and P_I = 19.1%. Respectively, for the MLC-based IMRT the P_+ value becomes 72.2% for a $\bar{\bar{D}}_B$ of 85.9 Gy having P_B = 87.8% and P_I = 15.5%.

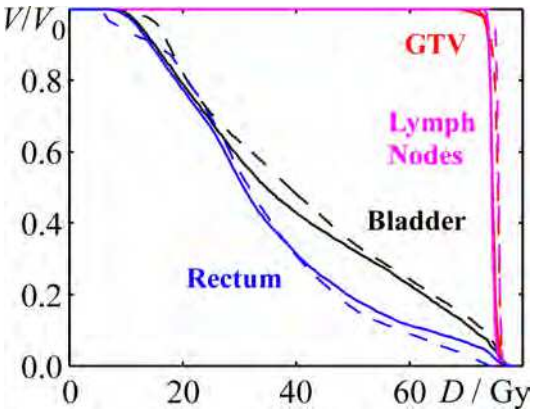

Fig. 8. The DVHs of the GTV and involved lymph nodes as well as those of the organs at risk (bladder and rectum) are illustrated. The solid lines correspond to the dose distribution from Helical Tomotherapy, whereas the dashed lines correspond to the dose distribution from IMRT (Mavroidis et al. 2007) (published with permission from: Mavroidis et al. Treatment plan comparison between Helical Tomotherapy and MLC-based IMRT using radiobiological measures. Physics in Medicine and Biology, Vol.52, pp. 3829, 2007, IOP Publishing Ltd, http://stacks.iop.org/PMB/52/3817).

The dose distribution in the ITV is more homogeneous in the MLC-based IMRT plan as compared to the HT, while achieving a similar sparing of the OARs. As it is shown in Fig. 9, the expected complication-free tumour control for the HT treatment plan is slightly worse than the MLC-based IMRT for the clinical prescribed doses. The reason for this is that the MLC-based IMRT irradiates more effectively the GTV and lymph nodes with better sparing of the rectum as shown in Table 2 and Fig. 9. Although the HT delivers similar mean dose to the rectum with a little larger variation as compared to the MLC-based IMRT, it shows a higher complication probability due to its higher maximum dose and the high relative seriality value of rectum (s = 0.7).

In this analysis, the clinical effectiveness of the Helical Tomotherapy and MLC-based IMRT in prostate cancer radiotherapy was evaluated using both physical and radiobiological criteria. This evaluation shows that the difference between the HT and MLC-based IMRT plans is small with the latter one being more effective over the clinically prescribed dose region. The results of this work indicate that the HT and MLC-based IMRT radiation

modalities have almost the same potential of producing treatment plans with small integral doses to the healthy organs and fairly homogeneous doses to the ITV.

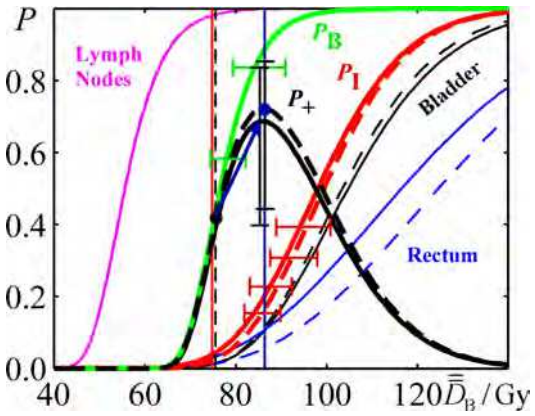

Fig. 9. The dose-response curves of the targets and organs-at-risk are plotted for the HT and MLC-based IMRT radiation modalities using the $\bar{\bar{D}}$ on the dose axis. The vertical lines denote the clinical and optimum dose prescriptions. The solid lines correspond to the dose distribution from Helical Tomotherapy, whereas the dashed lines correspond to the dose distribution from IMRT.

5. Radiobiological evaluation of optimized HDR prostate brachytherapy implants

High Dose Rate (HDR) Brachytherapy is becoming popular for treating localized prostate cancer tumors utilizing 3D ultrasound (U/S) and ^{192}Ir based remote afterloaders. Compared to other 3D imaging modalities (CT, MR) U/S can provide real-time, accurate 3D information on the size and the position of the target volume, on the position of the organs-at-risk and the real time needle tracking and navigation. The use of inverse planning in HDR brachytherapy results in a fast planning process that produces reproducible high quality treatment plans that closely match the clinical protocol constraints (Baltas & Zamboglou 2006, Hsu et al. 2008, Martinez et al. 1989, Milickovic et al. 2002). During the last decade a number of inverse planning algorithms have been proposed (Alterovitz et al. 2006, Karabis et al. 2009, Lahanas et al. 1999, 2003) and many of them have been implemented in modern Treatment Planning Systems (TPS) (Oncentra Prostate™, Nucletron B.V., Veenendaal, The Netherlands, Oncentra Brachy™, Nucletron B.V., Veenendaal, The Netherlands, BrachyVision Treatent Planning™, Varian Medical Systems). It is a common characteristic for HDR implants optimized with such algorithms that there are a few very dominating dwell positions, where the largest part of the total dwell time is spent, which leads to a selective extension of high doses in volumes around such dwell positions. Presently, in HDR brachytherapy, new inverse optimization algorithms enable an adjustment of the source dwell time distribution within the implanted catheters according to user-defined objectives and penalties for the target volume(s) and organs at risk (OARs).

In the present evaluation, the TPS Oncentra Prostate v.3.0 (Nucletron B.V., Veenendaal, The Netherlands) was used, where the Hybrid Inverse treatment Planning and Optimization (HIPO) algorithm has been implemented (Karabis et al. 2005, 2009). HIPO is an inverse planning algorithm that is based on 3D anatomy and it is capable of optimizing the dose distribution for a given needle configuration as well as finding an adequate needle configuration for each application. Furthermore, HIPO has the ability to apply a modulation restriction that limits the free modulation of dwell times eliminating the selective hot spots. It is based on dosimetric objectives, which penalize over/under dosage in target(s) while protecting OARs from overdosage (Karabis et al. 2009). Furthermore, in order to get restriction of the free modulation of dwell times allowing thus more smooth source movements and more smooth distributions of dwell time over dwell positions, HIPO offers the option of a modulation restriction (MR) parameter, which leads to a the dwell time gradient restriction.

The present analysis is based on the treatment plans of 12 prostate cancer patients, which were developed using their 3D ultrasound (U/S) image sets that were obtained intra-operatively right after the needle implantation. The twelve clinical implants for HDR brachytherapy of prostate cancer were selected as monotherapy for low-risk cases and they cover the whole range of prostate volumes with a full range of 26-101 cm^3. In the present clinical protocol, the HDR Monotherapy is delivered in three implants separated by at least 2 weeks interval. In each implant a single fraction with a prescription dose of 11.5 Gy is delivered thus resulting in a total dose of 34.5 Gy. The prostate gland is considered as PTV and urethra, bladder and rectum are used as OARs in the treatment planning. The whole procedure including dose delivery is realized intra-operatively utilizing 3D and 2D Ultrasound imaging.

For the evaluation and report of the quality of the dose distributions, the following DVH-based parameters that have been proposed by GEC/ESTRO-EAU (19-22), have been considered (Baltas & Zamboglou 2006, Kovács et al. 2005, Nag et al. 1999).

$\boldsymbol{D_{100}}$: The dose that covers 100% of the PTV volume, which is the Minimum Target Dose (MTD).

$\boldsymbol{D_{90}}$: The dose that covers 90% of the PTV volume, which would be desirable to be equal or greater than the prescription dose.

$\boldsymbol{V_{100}}$: The percentage of prostate volume (PTV) that has received at least the prescription dose (100% = prescribed dose).

$\boldsymbol{V_{150}}$: The volume that has received 50% more than the prescribed dose (150% of the prescription dose).

Regarding the OARs, the following dosimetric descriptors for the maximum doses have been considered:

$\boldsymbol{D_{2cm^3}}$: the dose for the most exposed 2 cm^3 of rectum or bladder,

$\boldsymbol{D_{0.1cm^3}}$: the dose for the most exposed 0.1cm^3 of the urethra as an estimate of the maximum dose

$\boldsymbol{D_{10}}$: the highest dose covering 10% of the OAR volume (rectum, bladder, urethra)

All the clinical implants have been inversely planned using HIPO with modulation restriction (MR), which was selected based on the maximum values resulting in plans that completely fulfilled the constraints of the dosimetric protocol. In the treatment plan evaluation, the individual tissue DVHs were calculated for each plan (Fig. 10).

The different treatment plans were further evaluated in conjunction with radiobiological dose non-uniformity evaluation measures in order to estimate their expected clinical impact

(Mavroidis et al. 2008). For this evaluation the dose-response parameters of the prostate, urethra, bladder and rectum (Table 3) were used to calculate the corresponding response probabilities as well as the complication-free tumor control probability (P_+) and the biologically effective uniform dose ($\bar{\bar{D}}$).

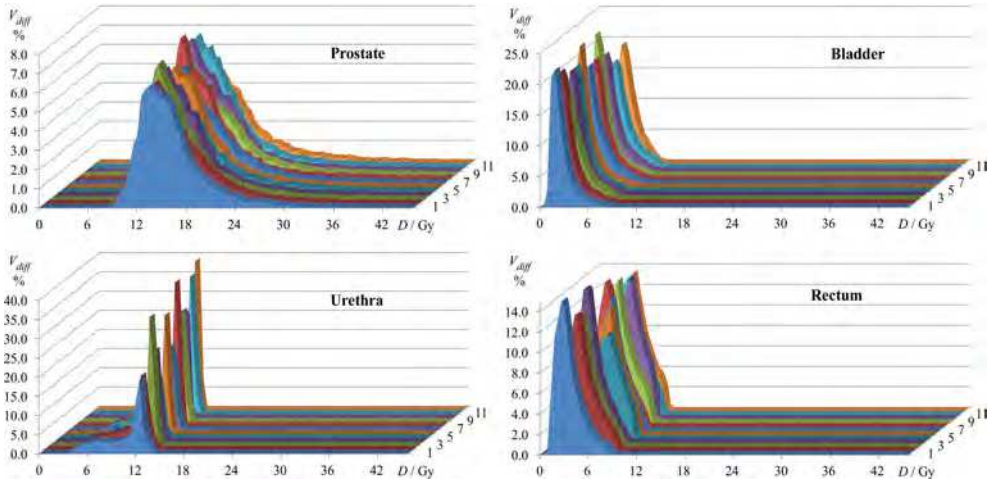

Fig. 10. The differential DVHs of prostate, urethra, bladder and rectum derived from the treatment plans. The prescription dose of the fraction is 11.5 Gy (100%).

Organs	D50 (Gy)	γ	s	α/β
PTV	70.0	4.0	–	3.0
Urethra	120.0	3.0	0.03	3.0
Bladder	80.0	3.0	0.3	3.0
Rectum	80.0	2.2	0.7	3.0

Table 3. Summary of the model parameter values for the prostate cancer cases. D_{50} is the 50% response dose, γ is the maximum normalized value of the dose-response gradient and s is the relative seriality, which characterizes the volume dependence of the organ.

Finally, the conformal index COIN (Baltas et al. 1998), which is a measure of brachytherapy implant quality and dose specification, was applied in evaluation of the examined treatment plans. COIN considers also the conformity of the 3D dose distribution regarding the OARs based on three coefficients. The first coefficient is the fraction of the PTV that is enclosed by the prescription dose. The second coefficient is the fraction of the volume encompassed by the prescription dose that is covered by PTV and it is a measure of how much tissue outside the PTV is covered by the prescription dose. The third coefficient is the fraction of the volume of each OAR that receives doses that exceed their dose limit.

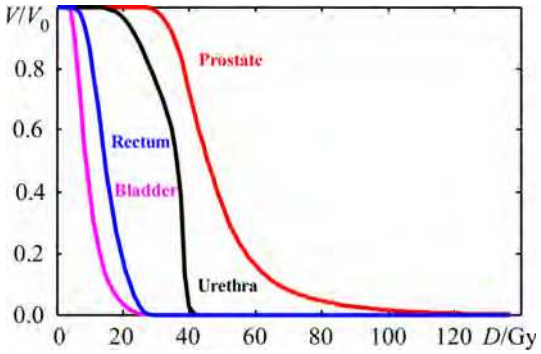

Fig. 11. The average cumulative DVHs of the PTV (prostate gland, red), urethra (black), bladder (pink) and rectum (blue) are presented for the HDR treatment plans, which were optimized with modulation restriction. Here, the total dose of 34.5 Gy delivered by three fractions of 11.5 Gy is considered to be the total prescription dose (100%) (Mavroidis et al. 2010) (published with permission from: Mavroidis et al. Radiobiological evaluation of the influence of dwell time modulation restriction in HIPO optimized HDR prostate brachytherapy implants. Journal of Contemporary Brachytherapy, Vol.2, pp. 126, 2010, Termedia sp.zo.o., DOI: 10.5114/jcb.2010.16923).

Fig. 11 illustrates the average DVHs of the dose distributions examined. Based on the DVHs and the results shown in Table 4, the HIPO optimization with MR has an acceptable variance coefficient, CV, (meaning dose inhomogeneity) inside the PTV. The average mean dose in the PTV in the HIPO with MR plans is 48.4 Gy and the corresponding control probability is 97.8%. Regarding the organs at risk, the HIPO optimization with MR plans deliver fairly low maximum doses in urethra, which results in a clinically acceptable response probability (3.8%) (Mavroidis et al. 2010).

Tissues	CTV	Urethra	Bladder	Rectum
P (%)	97.8	3.8	0.0	0.02
D_{mean} **(Gy)**	48.4	33.0	9.2	14.4
CV **(%)**	30.5	18.2	46.5	33.3
$\bar{\bar{D}}$ **(Gy)**	32.9	34.2	22.3	22.8
D_{max} **(Gy)**	136.6	41.4	27.6	27.6
D_{min} **(Gy)**	23.5	11.0	2.8	2.8

Table 4. Summary of the dosimetric and radiobiological measures averaged over the 12 prostate cancer patients regarding the applied HDR technique.

A quantitative analysis of the dosimetric and radiobiological results of the different dose distributions shows that for the HDR optimization with MR at the clinical dose prescription the P_+ value is 94.0% and the biologically effective uniform dose to the PTV, $\bar{\bar{D}}_B$ is 32.9Gy. The total control probability, P_B is 97.8% and the total complication probability, P_I is 3.8%, which mainly stems from the response probability of urethra (3.8%) (Mavroidis et al. 2010). However, if a different dose level of the dose distributions is selected in order to maximize

the complication-free tumor control then the P_+ value becomes 95.2% for a $\bar{\bar{D}}_B$ of 32.2 Gy having P_B = 96.3% and P_I = 1.1%.
The average COIN values, which were calculated with and without the inclusion of the organs at risk (OARs) for the 12 implants using HIPO with modulation restriction are 0.867 ± 0.019 and 0.870 ± 0.021, respectively. These values indicate that the examined treatment plans are characterized by high quality.

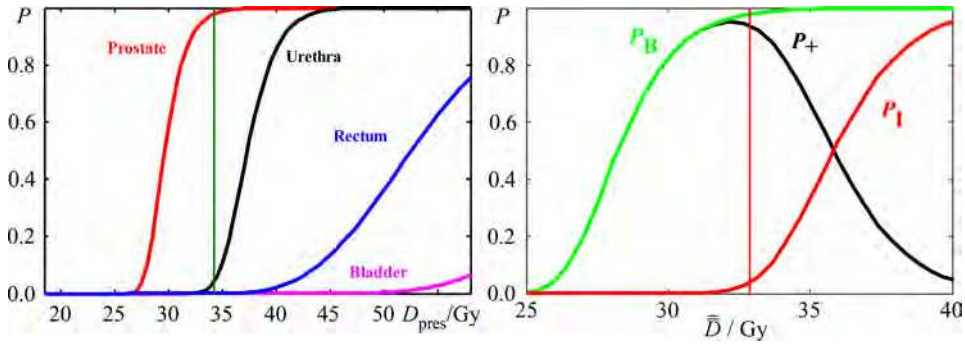

Fig. 12. *Left diagram:* The average dose-response curves of the PTV (red), urethra (black), bladder (pink) and rectum (blue) are presented for the HDR treatment plans, which were optimized with modulation restriction, regarding different prescription doses. *Right diagram:* The average curves of the total tumor control probability, P_B (green), total normal tissue complication probability, P_I (red) and complication-free tumor control probability, P_+ (black) are presented for the HDR treatment plans, regarding different radiobiological prescription doses. The total dose of 34.5 Gy delivered by three fractions of 11.5 Gy is considered to be the total prescription dose (100%) (Mavroidis et al. 2010) (published with permission from: Mavroidis et al. Radiobiological evaluation of the influence of dwell time modulation restriction in HIPO optimized HDR prostate brachytherapy implants. Journal of Contemporary Brachytherapy, Vol.2, pp. 126, 2010, Termedia sp.zo.o., DOI: 10.5114/jcb.2010.16923).

Non-uniform dose distributions, which may be as effective as equivalent uniform dose distributions, which means that a higher number of degrees-of-freedom can be taken advantage of by incorporating radiobiological measures in treatment plan optimization. In this sense, a radiobiologically based optimization algorithm could find dose distributions of smoother non-uniformity that irradiate the target as effectively as the physically optimized dose distributions without modulation restriction and at the same time optimize the dose fall-off towards the organs at risk. This is because the radiobiologically based HDR optimization would take into account the volume effect of all the involved organs at risk in the proximity of the target and optimize the dose fall-off accordingly. It has to be mentioned that radiobiologically based HDR optimization is characterized by more clinically relevant dose constraints for the OARs and normal tissue stroma, which could lead to better results than the HDR optimization without modulation restriction. However, the large hot spots produced in the target volume by this method would increase the risk for secondary cancer (Schneider et al 2006). Consequently, by deteriorating physical dose conformation, the HDR optimization with MR provides slightly better biological conformation.

6. Conclusions

This chapter demonstrates the use of radiobiological measures in prostate cancer treatment plan optimization may have a great impact on the clinical effectiveness of the applied treatment. Taking into account the dose-response relations of the irradiated tumors and normal tissues, a radiobiological dose delivery evaluation can be performed, which combines the information of a given dose distribution with the radiosensitivity map of the patient. The use of $P-\bar{\bar{D}}$ diagrams can complement the traditional tools of evaluation such as DVHs, in order to compare and effectively evaluate different treatment plans.

The findings show that the use of fused CT-MRI images produce dose distributions, which lead on average to better expected treatment outcome compared to the use of CT images alone. The extent of this improvement decreases as we move from conventional to IMRT treatments due to the fact that IMRT delivers already limited doses to OARs. Although 3D conformal radiotherapy techniques are not characterized by very high conformalities, the better knowledge of the CTV extension can considerably improve the effectiveness of their dose distributions. These findings were observed during treatment plan evaluation and comparison based on common dosimetric indices as well as on radiobiological measures.

The clinical effectiveness of delivered Helical Tomotherapy dose distributions with and without patient setup correction, which were evaluated using both physical and biological criteria, showed that the dose distributions with and without patient setup correction are very similar and the expected clinical outcome is not always better in the first case unless a radiobiological treatment plan optimization has been performed first. However, the effectiveness of a HT treatment plan can be considerably deteriorated if an accurate initial patient setup procedure is not available. The application of radiobiological measures on HT prostate cancer treatment plans with and without patient setup correction revealed minor or modest differences in the predicted therapeutic impact of using the MVCT method.

Radiobiological evaluation of treatment plans provides additional information about the fitness of a plan and a closer association of the delivered treatment with the clinical outcome. The simultaneous presentation of the radiobiological evaluation together with the physical data shows their complementary relation in analyzing a dose plan. The use of radiobiological parameters is necessary if a clinically relevant quantification of a plan is needed. The application of the P_+ and $\bar{\bar{D}}$ concepts on representative Helical Tomotherapy and MLC-based IMRT prostate cancer treatment plans revealed differences in the biological impact of the corresponding dose distributions. It can be concluded that for clinical cases, which may look dosimetrically similar, in radiobiological terms they can be quite different. Helical Tomotherapy and MLC-based IMRT can cover the target volume with the clinically prescribed dose while minimizing the volume of the organs at risk receiving high dose. Both radiation modalities have almost the same potential of producing treatment plans of equivalent clinical effectiveness in terms adequate irradiation of the tumor and sparing of the involved OARs.

At the maximum P_+ dose prescription, it was proved that the different modulation restriction approaches do not affect significantly the proper coverage and eradication of the target and the sparing of rectum and bladder but they affect mainly the effective sparing of urethra. In this analysis, which was performed using both physical and radiobiological criteria, it is shown that the HDR optimization with MR can introduce a minor improvement in the effectiveness of the produced dose distribution compared to the HDR optimization without modulation restriction. The likelihood to accomplish a good treatment result can be

increased by the use of therapeutic indices such as P_+ and $\bar{\bar{D}}$, which can be used as figures of merit for a treatment.

7. Appendix

Radiobiological treatment plan evaluation

In the present radiobiological treatment plan evaluation method, the Linear-Quadratic-Poisson model is used to describe the dose-response relation of the tumours and normal tissues (Källman et al. 1992b, Ågren et al. 1990). This model takes into account the fractionation effects that are introduced by the clinical protocol:

$$P(D) = \exp\left(-e^{e\gamma - (D/D_{50})\cdot(e\gamma - \ln\ln 2)}\right) \tag{1}$$

where $P(D)$ is the probability to control a tumour or induce a certain injury to a normal tissue that is irradiated uniformly with a dose D. D_{50} is the dose, which gives a 50% response and γ is the maximum normalized dose-response gradient. The parameters D_{50} and γ are specific for every organ and type of clinical endpoint and they are derived directly from clinical data (Emami et al. 1991, Eriksson et al. 2000, Gagliardi et al. 2000, Jackson et al. 1995, Mavroidis et al. 2003, 2005, Roesink et al. 2001, Willner et al. 2002, Ågren 1995). The uncertainties that are associated with these parameters are of the order of 5% for D_{50}, 30% for γ and 90% for s. These uncertainties define the confidence interval of the entire dose-response curve around its best estimate (Deasy 1997). The response of the entire organ to a non-uniform dose distribution is given by an expanded version of Eq. (1) for tumours and the relative seriality model for normal tissues (Lind et al. 1999).

The relative seriality model is a model that account for the volume effect. For a heterogeneous dose distribution, the overall probability of injury (P_I) for a number of OARs is expressed as follows (Källman et al. 1992b, Lind et al. 1999):

$$P_I = 1 - \prod_{j=1}^{N_{organs}} \left(1 - [1 - \prod_{i=1}^{M_j} (1 - P^j(D_i)^{s_j})^{\Delta v_i}]^{1/s_j}\right) \tag{2}$$

where P_I^j is the probability of injuring organ j and N_{organs} is the total number of vital OARs. $P^j(D_i)$ is the probability of response of the organ j having the reference volume and being irradiated to dose D_i as described by Eq. (1). $\Delta v_i = \Delta V_i / V_{ref}$ is the fractional sub-volume of the organ that is irradiated compared to the reference volume for which the values of D_{50} and γ were calculated. M_j is the total number of voxels or sub-volumes in the organ j, and s_j is the relative seriality parameter that characterizes the internal organization of that organ. A relative seriality close to zero ($s \approx 0$) corresponds to a completely parallel structure, which becomes non-functional when all its functional subunits are damaged, whereas $s \approx 1$ corresponds to a completely serial structure which becomes non-functional when at least one functional subunit is damaged. It should be mentioned that other models such as the LKB (Burman et al. 1991, Kutcher et al. 1991, Kwa et al. 1998), parallel (Boersma et al. 1995) etc could also have been used with the appropriate response parameter set.

Tumours are assumed to have a parallel structural organization since the eradication of all of the clonogenic cells is required. Furthermore, in complex multi-target cancer cases, the

eradication of all the clonogenic cells in tumours implies that every individual tumour has to be eradicated. This implication indicates a parallel organization fashion for the tumours. Taking this assumption into account the overall probability of tumour control (P_B), is given by the expression (Lind et al. 1999, Mavroidis et al. 2000):

$$P_B = \prod_{j=1}^{N_{\text{tumours}}} \left(\prod_{i=1}^{M_j} P^j(D_i)^{\Delta v_i} \right) \tag{3}$$

where P_B^j is the probability of eradicating tumour j and N_{tumours} is the total number of tumours or targets involved in the clinical case.

To evaluate the effectiveness of the treatment plans, the concept of P_+, which expresses the probability of achieving tumour control without causing severe damage to normal tissues (Källman et al. 1992a), was employed. Using the quantities P_B and P_I, which were defined above, the P_+ can be estimated from the following expression:

$$P_+ = P_B - P_{B\cap I} \approx P_B - P_I \tag{4}$$

This concept is based on the accuracy of the models to calculate the probabilities P_B and P_I and the radiobiological parameters, which describe the dose-response relations of the different tumours and normal tissues.

As a measure of the quality of a treatment plan, the mean doses and their standard deviations to the target volumes and organs at risk are usually reported, together with the minimum and maximum doses as well as some DVH-based constraints. In addition to those parameters, the present radiobiological treatment plan evaluation uses the $\bar{\bar{D}}$ concept, which is defined as the dose that causes the same tumour control or normal tissue complication probability as the actual dose distribution given to the patient and it is derived numerically from the following expression (Mavroidis et al. 2000, 2001):

$$P_B(\vec{D}) \equiv P_B(\bar{\bar{D}}_B) \tag{5}$$

where $\vec{D}$ denotes the 3-dimensional dose distribution. This definition is a generalization of the effective uniform dose, D_{eff} introduced by Brahme (Brahme 1984). By normalizing treatment plans to a common prescription point ($\bar{\bar{D}}$) and then plotting out the tissue response probability vs. $\bar{\bar{D}}$ curves, a number of plan trials can be compared based on radiobiological endpoints.

8. References

Alterovitz, R.; Lessard, E.; Pouliot, J.; Hsu, I.; O'Brien, J. & Goldberg, K. (2006). Optimization of HDR Brachytherapy Dose Distributions Using Linear Programming with Penalty Costs. *Medical Physics,* Vol.33, pp. 4012–4019

Baltas, D.; Kolotas, C.; Geramani, K.; Mould, R.F.; Ioannidis, G.; Kekchidi, M. & Zamboglou, N. (1998). A Conformal Index (COIN) to Evaluate Implant Quality and Dose Specification in Brachytherapy. *International Journal of Radiation Oncolology, Biology, Physics*, Vol.40, pp. 515-524

Baltas, D. & Zamboglou, N. (2006). 2D and 3D Planning in Brachytherapy, In: *New Technologies in Radiation Oncology,* of Bortfeld, T.; Grosu, A.-L. & Schlegel, W., pp. 237-254, Springer, Berlin-Heidelberg

Beasley, M.; Driver, D. & Dobbs, H.J. (2005). Complications of Radiotherapy: Improving the Therapeutic Index. *Cancer Imaging,* Vol.5, pp. 78-84

Boswell, S.; Tomé, W.; Jeraj, R.; Jaradat, H. & Mackie, T.R. (2006). Automatic Registration of Megavoltage to Kilovoltage CT Images in Helical Tomotherapy: An Evaluation of the Setup Verification Process for the Special Case of a Rigid Head Phantom. *Medical Physics,* Vol.33, pp. 4395

Brahme, A. (1994). Which parameters of the dose distribution are best related to the radiation response of tumours and normal tissues. *Proceedings of the Interregional Seminars for Europe, the Middle East and Africa Organized by the IAEA*, Leuven, pp. 37-58

Brahme, A. (1997). The Need for Accurate Target and Dose Specifications in Conventional and Conformal Radiation Therapy – An Introduction. *Acta Oncologica,* Vol.36, pp. 789-792

Buffa, F.M.; Davidson, S.E.; Hunter, R.D.; Nahum, A.E. & West, C.M. (2001). Incorporating Biologic Measurements (SF2, CFE) into a Tumor Control Probability Model Increases their Prognostic Significance: A Study in Cervical Carcinoma Treated with Radiation Therapy. *International Journal of Radiation Oncolology, Biology, Physics*, Vol.50, pp. 1113-1122

Chen, L.; Price, R.A. Jr.; Wang, L.; Li, J.; Qin, L.; McNeeley, S.; Ma, C.M.; Freedman, G.M. & Pollack, A. (2004). MRI-Based Treatment Planning for Radiotherapy: Dosimetric Verification for Prostate IMRT. *International Journal of Radiation Oncolology, Biology, Physics*, Vol.60, pp. 636-647

Claus, F.G.; Hricak, H. & Hattery, R.R. (2004). Pretreatment Evaluation of Prostate Cancer: Role of MR Imaging and 1H MR Spectroscopy. *Radiographics,* Vol.24, pp. S167-S180

Creutzberg, C.L.; Althof, V.G.M.; Huizenga, H.; Visser, A.G. & Levendag, P.C. (1993). Quality Assurance Using Portal Imaging: The Accuracy of Patient Positioning in Irradiation of Breast Cancer. *International Journal of Radiation Oncolology, Biology, Physics*, Vol.25, pp. 529-539

Debois, M.; Oyen, R.; Maes, F.; Verswijvel, G.; Gatti, G.; Bosmans, H.; Feron, M.; Bellon, E.; Kutcher, G.; Van Poppel, H. & Vanuytsel, L. (1999). The Contribution of Magnetic Resonance Imaging to the Three-Dimensional Treatment Planning of Localized Prostate Cancer. *International Journal of Radiation Oncolology, Biology, Physics*, Vol.45, pp. 857-865

Emami, B.; Lyman, J.; Brown, A.; Coia, L.; Goitein, M.; Munzenrider, J.E.; Shank, B.; Solin, L.J. & Wesson, A.M. (1991). Tolerance of Normal Tissue to Therapeutic Irradiation. *International Journal of Radiation Oncolology, Biology, Physics*, Vol.21, pp. 109-22

Fenwick, J.D. & Nahum, A.E. (2001). Series Model Volume Effects in a Population of Non-Identical Patients: How Low is Low? *Physics in Medicine and Biology,* Vol.46, pp. 1815-1834

Hou, A.H.; Swanson, D. & Barqawi, A.B. (2009). Modalities for Imaging of Prostate Cancer. *Advances in Urology,* 818065

Hsu, I-C.; Yamada, Y.; Vigneault, E. & Pouliot, J. (2008). *Prostate High-Dose Rate Task Group,* American Brachytherapy Society, Retrieved from www.americanbrachytherapy.org

Jackson, A.; Ten Haken, R.K.; Robertson, J.M.; Kessler, M.L.; Kutcher, G.J. & Lawrence, T.S. (1995). Analysis of Clinical Complication Data for Radiation Hepatitis Using a Parallel Architecture Model. *International Journal of Radiation Oncolology, Biology, Physics*, Vol.31, pp. 883-891

Karabis A, Giannouli S, Baltas D. (2005). HIPO: A Hybrid Inverse Treatment Planning Optimization Algorithm in HDR Brachytherapy. *Radiotherapy and Oncology,* Vol.76, Supplement 2, pp. S29

Karabis, A.; Belotti, P. & Baltas, D. (2009). Optimization of Catheter Position and Dwell Time in Prostate HDR Brachytherapy using HIPO and Linear Programming, *Proceedings of World Congress on Medical Physics and Biomedical Engineering,* Munich, Germany, September 7-12, 2009, pp. 612-615

Kovács, G.; Pötter, R.; Loch, T.; Hammer, J.; Kolkman-Deurloo, I-K.; de la Rosette, J.J.M.C.H. & Bertermann, H. (2005). GEC/ESTRO-EAU Recommendations on Temporary Brachytherapy Using Stepping Sources for Localised Prostate Cancer. *Radiotherapy and Oncology,* Vol.74, pp. 137–148

Källman, P.; Lind, B.K. & Brahme, A. (1992a). An Algorithm for Maximizing the Probability of Complication Free Tumor Control in Radiation Therapy. *Physics in Medicine and Biology,* Vol.37, pp. 871-890

Källman, P.; Ågren, A.K. & Brahme, A. (1992b). Tumor and Normal Tissue Responses to Fractionated Non Uniform Dose Delivery. *International Journal of Radiation Biology,* Vol.62, pp. 249-262

Lahanas, M.; Baltas, D. & Zamboglou, N. (1999). Anatomy-Based Three-Dimensional Dose Optimization in Brachytherapy Using Multiobjective Genetic Algorithms. *Medical Physics,* Vol.26, pp. 1904-1918

Lahanas, M.; Baltas, D. & Giannouli, S. (2003). Global Convergence Analysis of Fast Multiobjective Gradient Based Dose Optimization Algorithms for High-Dose-Rate Brachytherapy. *Physics in Medicine and Biology,* Vol.48, pp. 599-617

Lind, B.K.; Mavroidis, P.; Hyödynmaa, S. & Kappas, C. (1999). Optimization of the Dose Level for a Given Treatment Plan to Maximize the Complication Free Tumor Cure. *Acta Oncologica,* Vol.38, pp. 787-798

Löf, J.; Lind, B.K. & Brahme, A. (1995). Optimal Radiation Beam Profiles Considering the Stochastic Process of Patient Positioning in Fractionated Radiation Therapy. *Inverse Problems,* Vol.11, pp. 1189-1209

Mackie, T.R.; Balog, J.; Ruchala, K.J.; Shepard, D.; Aldridge, J.S.; Fitchard, E.E.; Reckwerdt, P.; Olivera, G.H.; McNutt, T. & Metha, M. (1999). TomoTherapy. *Seminars in Radiation Oncology,* Vol.9, pp. 108-117

Mavroidis, P.; Lind, B.K.; Van Dijk, J.; Koedooder, K.; De Neve, W.; De Wagter, C.; Planskoy, B.; Rosenwald, J.C.; Proimos, B.; Kappas, C.; Danciu, C.; Benassi, M.; Chierego, G. & Brahme, A. (2000). Comparison of Conformal Radiation Therapy Techniques Within the Dynamic Radiotherapy Project 'DYNARAD'. *Physics in Medicine and Biology,* Vol.45, pp. 2459-2481

Mavroidis, P.; Lind, B.K. & Brahme, A. (2001). Biologically Effective Uniform Dose ($\bar{\bar{D}}$) for Specification, Report and Comparison of Dose Response Relations and Treatment Plans. *Physics in Medicine and Biology,* Vol.46, pp. 2607-2630

Mavroidis, P.; Laurell, G.; Kraepelien, T.; Fernberg, J.O.; Lind, B.K. & Brahme, A. (2003). Determination and Clinical Verification of Dose-Response Parameters for

Esophageal Stricture from Head and Neck Radiotherapy. *Acta Oncologica,* Vol.42, pp. 865-881

Mavroidis, P.; al-Abany, M.; Helgason, A.R.; Ågren Cronqvist, A.K.; Wersäll, P.; Theodorou, K.; Kappas, C.; Lind, H.; Lind, B.K.; Steineck, G. & Brahme, A. (2005). Dose-Response Relations for Anal Sphincter Regarding Faecal Leakage and Blood or Phlegm in Stools After Radiotherapy for Prostate Cancer. *Strahlentherapie und Onkologie,* Vol.181, pp. 293-306

Mavroidis, P.; Costa Ferreira, B.; Shi, C.; Lind, B.K. & Papanikolaou, N. (2007). Treatment Plan Comparison Between Helical Tomotherapy and MLC-Based IMRT Using Radiobiological Measures. *Physics in Medicine and Biology,* Vol.52, pp. 3817-3836, © 2007 IOP Publishing Ltd, http://stacks.iop.org/PMB/52/3817

Mavroidis, P.; Komisopoulos, G.; Lind, B.K. & Papanikolaou, N. (2008). Interpretation of the Dosimetric Results of Three Uniformity Regularization Methods in Terms of Expected Treatment Outcome. *Medical Physics,* Vol.35, pp. 5009-5018

Mavroidis, P.; Katsilieri, Z.; Kefala, V.; Milickovic, N.; Papanikolaou, N.; Karabis, A.; Zamboglou, N. & Baltas, D. (2010). Radiobiological Evaluation of the Influence of Dwell Time Modulation Restriction in HIPO Optimized HDR Prostate Brachytherapy Implants. *Journal of Contemporary Brachytherapy,* Vol.2, pp. 117-128

Mavroidis, P.; Su, F.; Giantsoudi, D.; Stathakis, S.; Komisopoulos, G.; Shi, C.; Swanson G. & Papanikolaou, N. (2011). Radiobiological and Dosimetric Analysis of Daily Megavoltage CT Registration Techniques on Adaptive Radiotherapy with Helical Tomotherapy. *Technology in Cancer Research and Treatment,* Vol.10, pp. 1-13

Meeks, S.L.; Harmon Jr., J.F.; Langen, K.M.; Willoughby, T.R.; Wagner, T.H. & Kupelian, P.A. (2005). Performance Characterization of Megavoltage Computed Tomography Imaging on a Helical Tomotherapy Unit. *Medical Physics,* Vol.32, pp. 2673

Milickovic, N.; Lahanas, M.; Papagiannopoulou, M.; Zamboglou, N. & Baltas, D. (2002). Multiobjective Anatomy-Based Dose Optimization for HDR-Brachytherapy with Constraint Free Deterministic Algorithms. *Physics in Medicine and Biology,* Vol.47, pp. 2263-2280

Mitine, C.; Dutreix, A. & Van Der Schueren, E. (1991). Tangential Breast Irradiation: Influence of Technique of Set-Up on Transfer Errors and Reproducibility. *Radiotherapy and Oncology,* Vol.22, pp. 308-310

Martinez, A.A.; Orton, C.G. & Mould, R.F. (Eds.). (1989). *Brachytherapy HDR and LDR.* Nucletron International, B.V, Leersum, The Netherlands

Nag, S.; Beyer, D.; Friedland, J.; Grimm, P. & Nath, R. (1999). American Brachytherapy Society (ABS) Recommendations for Transperineal Permanent Brachytherapy of Prostate Cancer. *International Journal of Radiation Oncolology, Biology, Physics*, Vol.44, pp. 789-799

Parker, C.C.; Damyanovich, A.; Haycocks, T.; Haider, M.; Bayley, A. & Catton, C.N. (2003). Magnetic Resonance Imaging in the Radiation Treatment Planning of Localized Prostate Cancer Using Intra-Prostatic Fiducial Markers for Computed Tomography Co-Registration. *Radiotherapy and Oncology,* Vol.66, pp. 217-224

Rasch, C.; Barillot, I.; Remeijer, P.; Touw, A.; van Herk, M. & Lebesque, J.V. (1999). Definition of the Prostate in CT and MRI: a Multi-Observer Study. *International Journal of Radiation Oncolology, Biology, Physics*, Vol.43, pp. 57-66

Rørvik, J.; Halvorsen, O.J.; Espeland, A. & Haukaas, S. (1993). Inability of CT to Assess Local Extent of Prostate. *Acta Radiologica,* Vol.34, pp. 39–42

Scheidler, J.; Hricak, H.; Vigneron, D.B.; Yu, K.K.; Sokolov, D.L.; Huang, L.R.; Zaloudek, C.J.; Nelson, S.J.; Carroll, P.R. & Kurhanewicz, J. (1999). Prostate Cancer: Localization with Three-Dimensional Proton MR Spectroscopic Imaging Clinicopathologic Study. *Radiology* Vol.213, pp. 473-480

Tzikas, A.; Karaiskos, P.; Papanikolaou, N.; Stathakis, S.; Sandilos, P.; Koutsouveli, E.; Lavdas, E.; Scarleas, C.; Dardoufas, K.; Lind, B.K. & Mavroidis, P. (2011). Investigating the Clinical Aspects of Using CT vs. CT-MRI Images During Organ Delineation and Treatment Planning in Prostate Cancer Radiotherapy. *Technology in Cancer Research and Treatment,* Vol.10, pp. 231-42

Villeirs, G.M.; Van Vaerenbergh, K.; Vakaet, L.; Bral, S.; Claus, F.; De Neve, W.J.; Verstraete, K.L. & De Meerleer, G.O. (2005). Interobserver Delineation Variation Using CT Versus Combined CT+MRI in Intensity-Modulated Radiotherapy for Prostate Cancer. *Strahlentherapie und Onkologie,* Vol.181, pp. 424-430

Villeirs, G.M. & De Meerleer, G.O. (2007). Magnetic Resonance Imaging (MRI) Anatomy of the Prostate and Application of MRI in Radiotherapy Planning. *European Journal of Radiology*, Vol.63, pp. 361-368

Welsh, J.S.; Lock, M.; Harari, P.M.; Tomé, W.; Fowler, J.; Mackie, T.R.; Ritter, M.; Kapatoes, J.; Forrest, L.; Chappell, R.; Paliwal, B. & Mehta, M.P. (2006). Clinical Implementation of Adaptive Helical Tomotherapy: A Unique Approach to Image-Guided Intensity Modulated Radiotherapy. *Technology in Cancer Research and Treatment,* Vol.5, pp. 465-480

Webb S. (2000). *Intensity-Modulated Radiation Therapy*, IOP Publishing, Bristol, UK

Weinreb, J.C.; Blume, J.D.; Coakley, F.V.; Wheeler, T.M.; Cormack, J.B.; Sotto, C.K.; Cho, H.; Kawashima, A.; Tempany-Afdhal, C.M.; Macura, K.J.; Rosen, M.; Gerst, S.R. & Kurhanewicz, J. (2009). Prostate Cancer: Sextant Localization at MR Imaging and MR Spectroscopic Imaging Before Prostatectomy--Results of ACRIN Prospective Multi-Institutional Clinicopathologic Study. *Radiology* Vol.251, pp. 122-133

Ågren, A.-K.; Brahme, A. & Turesson, I. (1990). Optimization of Uncomplicated Control for Head and Neck Tumors. *International Journal of Radiation Oncolology, Biology, Physics*, Vol.19, pp. 1077-1085

Ågren, A.K. (1995). *Quantification of the response of heterogeneous tumors and organized normal tissues to fractionated radiotherapy, PhD Thesis,* Stockholm University, Stockholm, Sweden

Prostate Cancer - Diagnostic and Therapeutic Advances
Edited by Dr. Philippe E. Spiess

ISBN 978-953-307-319-4
Hard cover, 378 pages
Publisher InTech
Published online 25, November, 2011
Published in print edition November, 2011

In this book entitled "Prostate Cancer - Diagnostic and Therapeutic Advances", we highlight many of the significant advances made in our treatment armamentarium of prostate cancer. The book is subdivided into four sections termed: 1) novel diagnostic approaches, 2) surgical treatments options, 3) radiation therapy and its potential sequelae, and 4) medical management and its treatment complications. After reading the present book , readers will be very familiar with the major clinical advances made in our multifaceted treatment approach to prostate cancer over the past decade.This book is a tribute to our pioneering urologists and allied healthcare professionals who have continually pushed forward our traditional therapeutic envelope.

How to reference
In order to correctly reference this scholarly work, feel free to copy and paste the following:

Panayiotis Mavroidis, Dimos Baltas, Bengt K. Lind and Nikos Papanikolaou (2011). Use of Radiobiological Modeling in Treatment Plan Evaluation and Optimization of Prostate Cancer Radiotherapy, Prostate Cancer - Diagnostic and Therapeutic Advances, Dr. Philippe E. Spiess (Ed.), ISBN: 978-953-307-319-4, InTech, Available from: http://www.intechopen.com/books/prostate-cancer-diagnostic-and-therapeutic-advances/use-of-radiobiological-modeling-in-treatment-plan-evaluation-and-optimization-of-prostate-cancer-rad

INTECH
open science | open minds

InTech Europe
University Campus STeP Ri
Slavka Krautzeka 83/A
51000 Rijeka, Croatia
Phone: +385 (51) 770 447
Fax: +385 (51) 686 166
www.intechopen.com

InTech China
Unit 405, Office Block, Hotel Equatorial Shanghai
No.65, Yan An Road (West), Shanghai, 200040, China
中国上海市延安西路65号上海国际贵都大饭店办公楼405单元
Phone: +86-21-62489820
Fax: +86-21-62489821